Transactions of the **14th International Conference on Structural Mechanics in Reactor Technology** (SMiRT 14), Lyon, France, August 17-22, 1997 **GW/13**

Modelling the ductile tearing of austenitic welded joint with local approach of fracture

Devaux J.[1], **Joly P.**[1], **Leblond J.B.**[2]
(1) Framatome, France
(2) Université Pierre et Marie Curie Paris VI, France

ABSTRACT

This paper is devoted to the modelling of the ductile tearing of an austenitic weld with a modified Gurson-Tvergaard model. Toughness tests performed on the weld on CT25 and CT200 specimens were simulated. The simulations can correctly reproduce the much higher J-Δa resistance curve of the CT200 with respect to the CT25. This difference is due to an effect of specimen size, and to the lower tensile properties of the base metal which induce in the CT200 a large plastic deformation near the pin hole.

I. INTRODUCTION

The standard method to characterize and analyse the ductile crack initiation and growth in materials and structures is based on the J-Δa resistance curve. The limitations of this approach are now well known and are related to modifications of the stress triaxiality and the strain field at the crack tip, especially when conditions of general plasticity are reached in the structure. For Leak Before Break applications analysis of cracks in welds of austenitic pipes, the method requires the knowledge of resistance curves for ductile tearing on long distances. This kind of data cannot be obtained easily with laboratory specimen of reasonable size. Furthermore, the mismatch between weld and base metal tensile properties of austenitic materials makes difficult the interpretation of standard J-Δa resistance curve characterization of welds and its application to structures. The local approach of fracture can cope with these difficulties.
This paper is devoted to the application of an improved Gurson-Tvergaard model for simulating crack growth in an austenitic weld.
First, fracture toughness experiments performed on two types of specimens, CT25 and large CT 200 specimens, are described.
Then, the parameters of the model are identified following a specially qualified procedure [1]. Finally, the model is applied to the simulation of the crack growth in the large CT 200 specimen. The important effect of the specimen size on the measured J-Δa curve is reproduced and the limitations of the validity of the J calculations are discussed.

II MATERIALS AND EXPERIMENTAL RESULTS.

a- Materials

Toughness tests were carried out an austenitic weld. The base metal is a 316 L grade plate of 70 mm of thickness. The weld was fabricated by the SAW process with a 308 L type of welding product.
The chemical composition of both base and weld metals are given in table 1.

	C	Mn	Si	S	P	Ni	Cr	Mo	Cu	N	O
Base	0.010	1.45	0.36	0.001	0.019	11.16	18.20	2.78	0.080	0.054	0.068
Weld	0.020	1.78	0.48	0.002	0.027	12.48	17.93	2.40	0.36	0.07	

Table 1: Chemical compositions of the base and weld metals.

b- Tensile properties

Tensile properties are determined at room temperature for both base and weld metals. In the weld, tests are performed with tensile specimens entirely included in the weld metal in the transverse direction. The results of the tensile tests are given in table 2.

Material	Temp. (ºC)	position orientation	RP0.2 (MPa)	UTS (MPa)	A (%)	Z (%)
Base Metal	20	1/4T	258	554	70	83
		Transverse	260	561	72	84
weld metal	20	Top-T	505	633	29.	69
		1/2T-T	513	638	26	69
		Root-T	477	600	26	73

T=Transverse direction with respect to the welding direction

table 2: Tensile properties of the base and weld metals.

c- Ductile tearing resistance characterization

Two types of specimens are used for the toughness tests : a standard CT 25 and a CT 200 type of specimen with the full thickness of the weld (65 mm).
Standard CT 25 specimens with 20% side grooves are taken from the root and the top parts of the weld. They are oriented in the T-L directions and the crack front is centered on the weld center line. They are tested at 20ºC, and the J-Δa resistance curve is obtained by the method of partial unloading. The results of these tests are illustrated in figure 1a.
One large CT specimen was also tested. Its in plane dimensions are equivalent to those of a CT 200 (i.e. W=400 mm, H=480 mm), but its thickness is limited to the full thickness of the weld (65 mm).The specimen is 20% side grooved.
This test is performed at 20ºC and the J-Δa resistance curve is also determined also by the partial unloading method.
The crack length is determined either by simple or double compliance method. The two techniques give slightly different results. Thus, the J-Δa curves are given by a scatter band, which is illustrated in figure 1b. The range of crack extension obtained with this type of specimen is much larger than on the small CT 25 specimen ($\Delta a \geq 100$ mm against only ≈ 3 mm for the CT 25). Furthermore we can see on figure 1b that the J-Δa curve is much higher for the large specimen than for the CT25.

III DUCTILE FRACTURE MODELLING

a- Modified Gurson Model

To simulate the ductile fracture of the stainless weld metal, a modified Gurson-Tvergaard model [2-3] is used. It is based on the use of constitutive equations for plastic porous materials representing the growth and coalescence of micro-cavities. It is derived from the micromechanical analysis of a volume element of material surrounding one cavity. This model, improved by Leblond et al. is also described in reference [4]. The main parameters are the following : the initial volumic fraction of cavities f_0, the critical fraction of cavities corresponding to the onset of coalescence f_c, a parameter δ characterizing the rate of coalescence of the cavities, and the stress-strain relation.
All calculations using this model are performed by the SYSTUS finite element code developped by FRAMASOFT+CSI.
A method for identifying the main parameters f_c and δ, is described in reference [1] and [4].

b- Identification of the model parameters

1- Experiments
The procedure for identifying f_c and δ uses round notched tensile specimens. Such specimens, with a minimum diameter of 10 mm, a notch radius R of 10 mm (2 specimens), 4 mm (10 specimens) or 2 mm (2 specimens), and a shaft diameter of 18 mm, are tested at 20°C in the transverse direction in the top part of the weld (all the notch is contained in the weld metal). The applied load, the elongation and the reduction of the minimum notch diameter are recorded until fracture of the specimen.

2- Numerical simulations of notched round specimens
These round notched specimens are simulated with the model described above. The parameters needed for these simulations are the following : the initial volumic fraction of cavities f0 is equal to the volumic fraction of inclusions. The population of inclusions was studied by metallographical methods. They are mainly oxydes with a mean size of 4 μm and their volumic fraction was estimated to be $f_0=10^{-4}$.
The stress-strain relation was determined with the tensile tests in the transverse direction mentionned above.
The parameters f_c and δ must be determined by a trial-error technique. The effect of these parameters on the load-elongation curve or load-diametral contraction curve is described in references [1][4]. The simulation of such specimens (in particular the load-elongation curve up to failure initiation) does not depend on the mesh size.
Computed load-elongation curve on specimens with R=4 mm are illustrated in figure 2 (with an example of the mesh), compared to the scatter band of experimental curves. A good correspondance between simulations and experiments was obtained for $f_c=2.10^{-4}$ and $\delta=5.5$. These results are also confirmed by simulating the specimens with a notch radius R of 10 mm or 2 mm.
In order to use the model for simulating cracked structures, the very large gradient of volumic fraction of cavities f ahead of the crack tip makes the results of the computation dependant on the mesh refinement at the crack tip. It is shown in reference [1] that the mesh size can be regarded as an adjustable parameter, which completes the model so that it can be used for different sizes and geometries of cracked structures.

3- Numerical simulation of the CT25 specimen
The adjustment of the mesh size is performed by simulating the side grooved CT 25 specimen. The computation was a 2D plane strain simulation, with two rows of square

elements ahead of the crack tip on each side of the crack plane. The following mesh sizes are studied: 0.4 mm, 0.7 mm, 0.8 mm, and 1.0 mm. Because of the relative size of the weld groove with respect to the specimen size, the whole specimen is regarded to be made of weld metal. In figure 3, the the simulated results of load versus opening displacement are shown with the experimental curves. The computation of the load from the 2D simulation uses the apparent thickness (corrected of the effect of the side grooves) of 21.46 mm.
The wavy form of the curve is related to the successive unloading of the elements ahead of the crack tip due to their loss of carrying capaciy induced by damage. Results with mesh size of 0.7 mm to 1.0 mm are close to the experimental results.
The crack initiation and growth analysis is performed by computing J in the same way as for the experiments, from the area under the load displacement curve, and Δa from the length of the fully damaged zone. An example of fully damaged zone is illustrated in figure 4. With this method, the best adjustment of the J-Δa curve is obtained with the mesh size of 0.7 mm. The corresponding J-Δa curve compared to the experimental results is shown in figure 4 too.

IV SIMULATION OF THE LARGE CT 200 SPECIMEN

a- Results

2D simulations of the large CT 200 specimen are performed with the set of parameters identified in the previous sections. In order to save computation time the refined mesh size is extended only over 35 mm ahead of the crack tip (see figure 5). Computations are performed considering the two different materials in the specimen: the 308L weld metal covering a band of 36 mm of width, centered on the crack plane, and the base metal on each side of the weld metal. Results of load versus opening displacement derived from the plane strain calculation were adjusted on the experimental results with an apparent thickness of $B^* = 49.5$ mm. It is slightly lower than the usual estimation of B^* for plane strain of 55.8 mm because most of the specimen is in a state of stress between plane strain and plane stress.
As for the CT25 mentionned above, the J-Δa curve on the CT 200 specimen was derived from the area under the load-opening displacement curve for J, and from the length of the fully damaged zone for Δa. The J-Δa curve obtained with this method in the range of Δa which was computed ($\Delta a \leq 35$ mm) is illustrated in figure 5, compared to the experimental results.

b-Discussion

One can see in figure 5 that there is good correspondance between the experimental and the numerically computed J-Δa curves. In particular, the model can reproduce quantitatively the difference of resistance curve between the two specimens.
Furthermore it is possible to find elements of explanation for this difference. The J values were also computed for both types of CT specimens, by the direct path integral formula. As already mentionned in ref. [1], after crack initiation, the volume enclosed by the path must be large enough with respect to the volume of unloaded fully damaged material for J to become independant of the path.
For the CT25, one can see in figure 4 that the J values determined by the path integral or by the area under the load displacement curve are almost identical.
In the case of the CT 200, the situation is different, for at least two reasons:

- first there can be a specimen size effect. Calculation of the CT 200 entirely made of 308 L weld metal, as for the CT25, was performed to put this size effect in evidence. In figure 5, the results show that the resistance curve of the CT200 specimen is indeed

slightly higher than for the CT25. Up to crack extension of nearly 3.0 mm, the path integral is in good agreement with the J values deduced from the load curve, and is clearly higher than for the CT25 specimen. This illustrates the contribution of the size effect to the difference between the two specimens.

- the second reason comes from the mismatch effect between the weld and base metal properties. As it is illustrated in figure 6, very rapidly after crack initiation a plastic zone spreads through the softer base metal from the crack tip area to the pin hole and the upper surface of the specimen. Any further opening displacement then tends to plastify the pin hole area rather than to open the crack. For this reason, the apparent J derived from the load curve is higher than the actual J derived from the path integral (see figure 5). Nevertheless, as we can expect, the later is very similar to that calculated in the case of an homogeneous specimen of the same size. This tends to prove that in this case, the mismatch effect has little effect on the J-Δa curve, as long as J is computed locally around the crack tip, but it has a strong effect when J is derived from the load curve which integrates an additional displacement due to the large plasticity in the base metal. This displacement is clearly illustrated on the deformed geometry in figure 6.

V CONCLUSIONS

- Toughness tests are carried out on an austenitic weld, with CT25 and CT200 specimens. The results show that the J-Δa curve obtained on the CT200 is much higher than on the CT25.
- A modified Gurson-Tvergaard model is used to simulate the toughness experiments on the CT200 specimen. The parameters of the model are identified by simulating tests on round notched tensile and CT25 specimens.
- The simulated J-Δa curve on the bi-material CT200 is in very good agreement with the experimental data points, and reproduces the difference in J-Δa curve between the CT25 and the CT200.
- The explanation for this difference is twofold:

First, a simulation of a CT200 entirely of weld metal, shows that there is a small size effect between an homogeneous CT25 and a similar CT200.

Then, in the bi-material specimen, J derived from the load-opening displacement curve is larger because of the large plasticity near the pin hole in the softer base metal.

REFERENCES

1. Devaux,J., Joly,P., Leblond, J.B., 1995, Simulation by the local approach of the ductile crack growth in a pressure vessel steel using an improved Gurson Tvergaard model.
Proc. 21st MPA Seminar.
2. Gurson, A.L., 1977, Continuum theory of ductile rupture by void nucleation and growth : Part1. Yield criterion and flow rules for porous ductile media.
ASME Journal of Engineering Materials and Technology, 99 : 2-15.
3. Tvergaard,V., 1981, Influence of voids on shear band instabilities under plane strain conditions.
International Journal of Fracture,17: 389-407.
4. Leblond, J. B., Devaux,J. 1997, Advances in the numerical simulation of ductile fracture, paper 829.
Proc. of the 14th SMIRT.

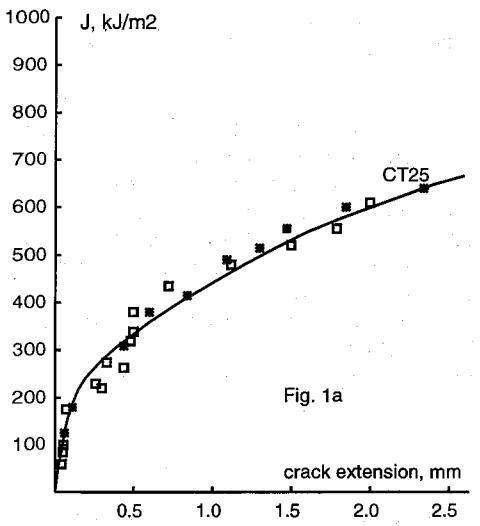

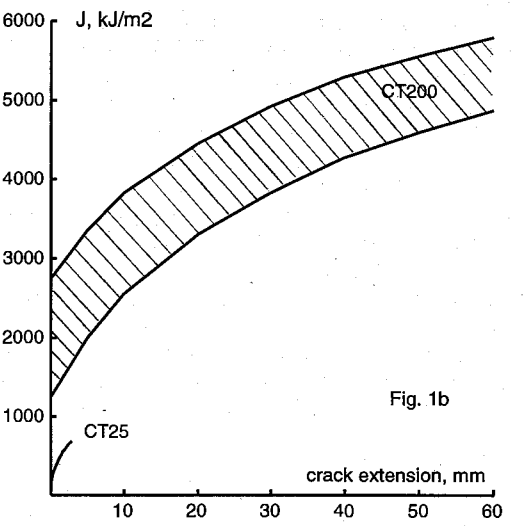

Figure 1 : Experimental resistance curves for the weld metal (1a : CT25 - 1b : CT200)

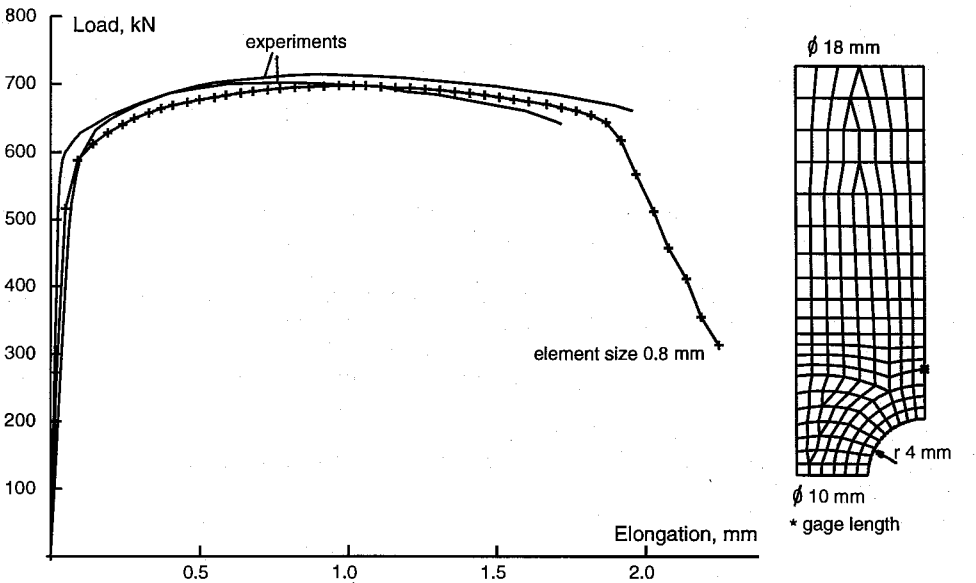

Figure 2 : Simulated and experimental results of load versus elongation for notched specimen in the weld metal

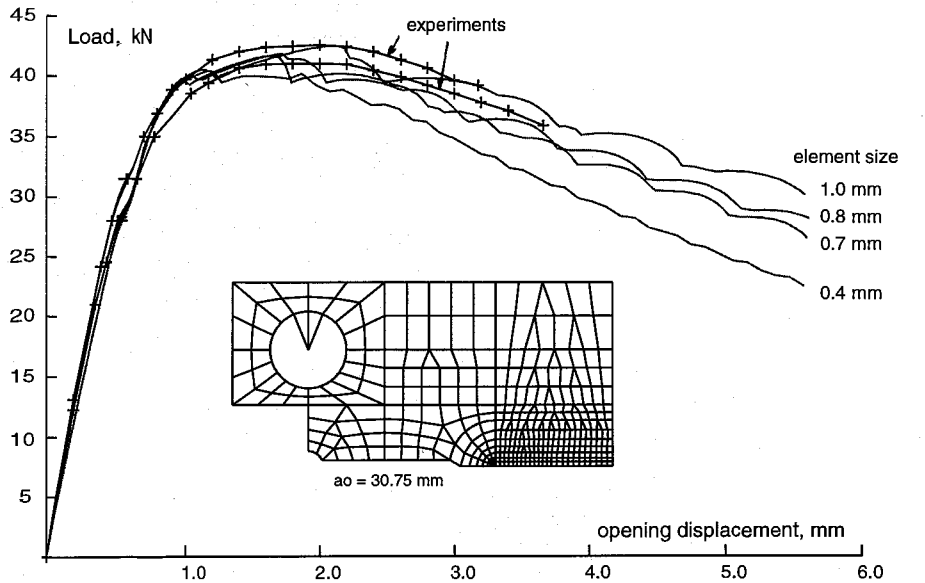

Figure 3 : Simulated and experimental results load versus opening displacement for CT25 specimen (weld metal)

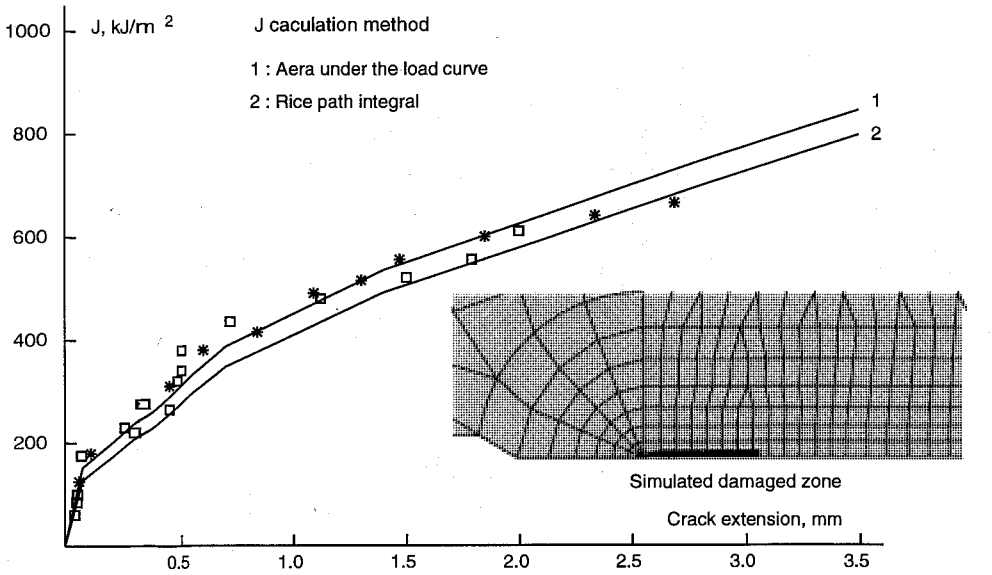

Figure 4 : Simulated resistance curves on CT25 specimen and experimental data points

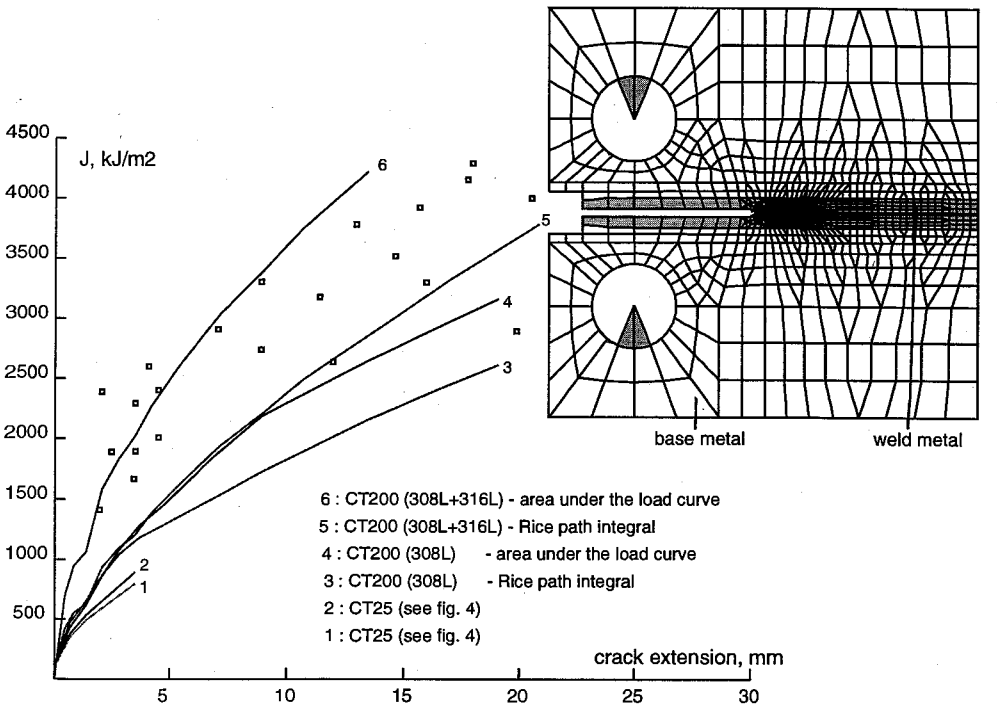

Figure 5 : Simulated resistance curves of CT200 and CT25 specimens

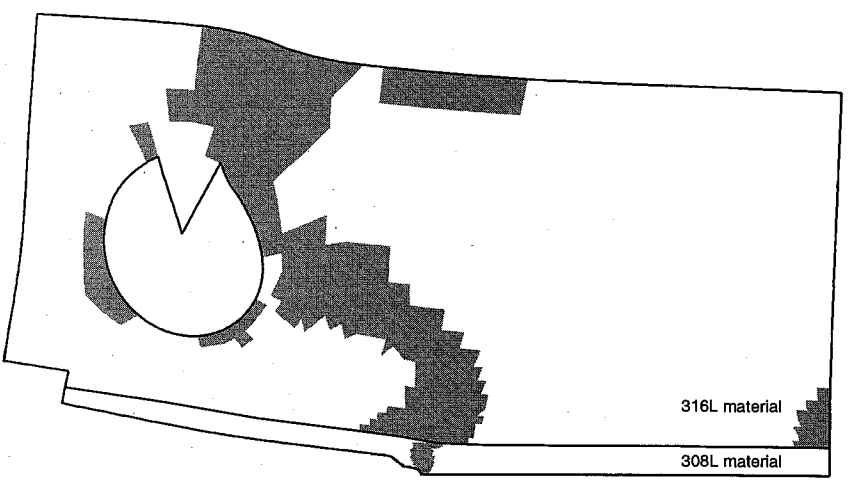

Figure 6 : Plastic zone in the CT200 specimen and deformed geometry(x 20) just after initiation

Conception XEROX BUSINESS SERVICES
Achevé d'imprimer en Juillet 1997 par l'Imprimerie Bayeusaine, 14401 Bayeux - Dépôt légal : Juin 1997